Cre recombinase-mediated restoration of nigrostriatal dopamine in dopamine-deficient mice reverses hypophagia and bradykinesia

Thomas S. Hnasko*, Francisco A. Perez*, Alex D. Scouras†, Elizabeth A. Stoll*, Samuel D. Gale*, Serge Luquet‡, Paul E. M. Phillips§, Eric J. Kremer¶, and Richard D. Palmiter†‡‖

*Graduate Program in Neurobiology & Behavior, Departments of †Biochemistry and §Psychiatry and Behavioral Sciences and Pharmacology, and ‡Howard Hughes Medical Institute, University of Washington, Seattle, WA 98195; and ¶L'Institut de Génétique Moléculaire de Montpellier, Centre National de la Recherche Scientifique, Unité Mixte de Recherche, 5535 Montpellier, France

Contributed by Richard D. Palmiter, April 18, 2006

A line of dopamine-deficient (DD) mice was generated to allow selective restoration of normal dopamine signaling to specific brain regions. These DD floxed stop (DDfs) mice have a nonfunctional *Tyrosine hydroxylase* (*Th*) gene because of insertion of a *Neo*^{R} gene flanked by lox P sites targeted to the first intron of the *Th* gene. DDfs mice have trace brain dopamine content, severe hypoactivity, and aphagia, and they die without intervention. However, they can be maintained by daily treatment with L-3,4-dihydroxyphenylalanine (L-dopa). Injection of a canine adenovirus (CAV-2) engineered to express Cre recombinase into the central caudate putamen restores normal *Th* gene expression to the midbrain dopamine neurons that project there because CAV-2 efficiently transduces axon terminals and is retrogradely transported to neuronal cell bodies. Bilateral injection of Cre recombinase into the central caudate putamen restores feeding and normalizes locomotion in DDfs mice. Analysis of feeding behavior by using lickometer cages revealed that virally rescued DDfs mice are hyperphagic and have modified meal structures compared with control mice. The virally rescued DDfs mice are also hyperactive at night, have reduced motor coordination, and are thigmotactic compared with controls. These results highlight the critical role for dopamine signaling in the dorsal striatum for most dopamine-dependent behaviors but suggest that dopamine signaling in other brain regions is important to fine-tune these behaviors. This approach offers numerous advantages compared with previous models aimed at examining dopamine signaling in discrete dopaminergic circuits.

canine adenovirus | feeding behavior | locomotor behavior | viral gene transfer | tyrosine hydroxylase

The dopamine neurons in the substantia nigra pars compacta (SNc) and ventral tegmental area (VTA) comprise about two-thirds of the dopaminergic neurons in the CNS (1, 2). These midbrain dopamine neurons send dense projections to forebrain structures, including the caudate putamen (CPu), nucleus accumbens (NAc), and olfactory tubercle, as well as sparser projections to the prefrontal cortex, amygdala, and hippocampus (2). These dopaminergic circuits have been implicated in a variety of fundamental mammalian behaviors such as movement, feeding, reward responses, and learning (for review, see refs. 3–6).

Dopamine-deficient (DD) mice (7) have been a useful genetic model to study the role of dopamine in these behaviors. DD mice are indistinguishable from littermates until ≈10 days, when they begin to manifest reduced body weight (BW) compared with controls, and, without intervention, DD mice will starve at ≈3 weeks (7). However, daily L-3,4-dihydroxyphenylalanine (L-dopa) treatment restores dopamine to the brain and induces ≈8 h of hyperactivity during which the DD mice consume enough food to survive (7, 8). This ability to temporarily restore dopamine signaling with L-dopa is the primary advantage of the DD mouse model compared with the 6-hydroxydopamine-lesion model because it allows us to test the mice in either a dopamine-depleted or dopamine-repleted state (9–11).

The most dramatic behavioral deficits in adult DD mice are their severe hypophagia and bradykinesia. We have demonstrated that these two phenotypes are dissociable by using viral-mediated gene transfer to restore dopamine synthesis to specific brain regions (12). This technique has allowed us to access the role of dopamine in discrete brain regions in mediating specific behaviors. Previously, we used recombinant adeno-associated viruses to promote synthesis of L-dopa within non-dopaminergic cells of the CPu or NAc (12, 13). Although this approach is effective, the viral-driven expression of *Tyrosine hydroxylase* (*Th*) in nondopaminergic neurons is artificial. Here we describe a genetic mouse model [DD floxed stop (DDfs)] in which the action of Cre recombinase delivered by a canine adenovirus (CAV-2) vector (14) allows expression of the endogenous *Th* gene. We use this model to ask whether restoration of dopamine signaling throughout the CPu is sufficient to restore normal feeding and locomotor behaviors.

Results

Canine Adenovirus Expressing Cre Recombinase (CAVCre)-Mediated Viral Rescue. Mice with a *Th* floxed stop (*Th*$^{fs/+}$) allele were generated with a *Pgk-Neo*^{R} cassette flanked by lox P sites targeted to the first intron of the *Th* locus. DDfs mice were generated by breeding *Th*$^{fs/+}$ mice with mice carrying a copy of the *Th* gene targeted to the *Dopamine β-hydroxylase* locus (*Dbh*$^{Th/+}$) to allow dopamine synthesis in noradrenergic cells (see Fig. 6, which is published as supporting information on the PNAS web site). The *Pgk-Neo*^{R} cassette effectively disrupts *Th* expression, as revealed by the fact that DDfs mice are severely hypoactive, aphagic, and are phenotypically indistinguishable from the original DD line as measured by basal motor activity, L-dopa induced locomotion (data not shown), and tissue dopamine content (see Table 1, which is published as supporting information on the PNAS web site).

To restore dopamine synthesis to specific dopaminergic circuits, CAVCre was injected bilaterally into the central region of the CPu. CAV-2 vectors are efficiently taken up by dopaminergic terminals and retrogradely transported to dopaminergic cell bodies where CAVCre drives expression of Cre recombinase

Conflict of interest statement: No conflicts declared.

Freely available online through the PNAS open access option.

Abbreviations: BW, body weight; CAVCre, canine adenovirus expressing Cre recombinase; CPu, caudate putamen; DD, dopamine-deficient; NAc, nucleus accumbens; rm, repeated measures; SNc, substantia nigra pars compacta; *Th*, *Tyrosine hydroxylase*; fs, floxed stop; vrDDfs, virally rescued DDfs; VTA, ventral tegmental area.

‖To whom correspondence should be addressed at: University of Washington, Howard Hughes Medical Institute, Box 357370, Seattle, WA 98195. E-mail: palmiter@u.washington.edu.

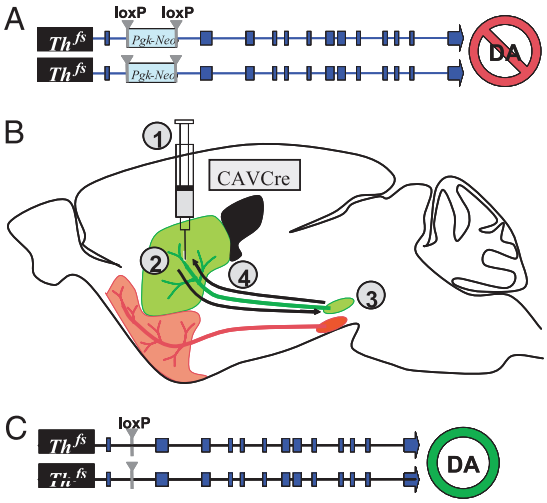

Fig. 1. Illustration of viral rescue strategy to restore *Th* production to dopamine neurons in DDfs mice ($Th^{fs/fs}$; $Dbh^{Th/+}$) (see Fig. 6 for more details). (*A*) Before viral rescue, DDfs mice have a *Pgk-NeoR* cassette flanked by lox P sites disrupting expression of the *Th* gene. (*B*) 1, CAVCre is injected into the central CPu (dashed circle approximates extent of viral spread); 2, CAVCre transduces local axon terminals near the site of injection, including those of midbrain dopamine neurons; 3, CAVCre is retrogradely transported to the dopamine cell bodies where it drives expression of Cre recombinase leading to the excision of the stop cassette allowing expression of the endogenous *Th* gene; 4, *Th* is then transported to the axon terminals of the infected dopaminergic neurons where it synthesizes L-dopa. CAVCre is retrogradely transported to cortical glutamatergic neurons as well, but recombination in those neurons is inconsequential because the *Th* gene is not expressed in those cells. (*C*) After Cre recombinase-mediated excison of the *Pgk-NeoR* cassette, *Th* expression and dopamine production are restored.

(14–16). CAVCre can excise the floxed $Pgk\text{-}Neo^R$ gene that disrupts the endogenous *Th* gene, thereby restoring dopamine production to those dopamine neurons that project to the central CPu (Fig. 1). As expected based on our previous work (12, 13, 17), this treatment rescued feeding and was sufficient to allow the DDfs mice to thrive in the absence of L-dopa. The effect is permanent because the endogenous *Th* gene is activated; virally rescued DDfs (vrDDfs) mice remained viable for >1 year without L-dopa.

Th expression was restored to many cell bodies of the SNc as well as to a few VTA neurons in the vrDDfs mice (Fig. 2 *A–F*). Despite the fact that the site of viral transduction is restricted to the central region of the CPu (12, 18), vrDDfs mice had widespread expression of *Th* throughout the CPu (Fig. 2*I*), presumably because of the central site of injection and extensive arborization of dopamine axons. *Th* immunostaining was restored throughout the dorsal and ventrolateral striatum; staining was also occasionally observed in the lateral olfactory tubercle but not in the medial NAc core or shell (Fig. 2 *G–L*; for images with the dopamine transporter signal removed, see Fig. 7, which is published as supporting information on the PNAS web site). In DDfs (and DD) mice, striatal cells bearing dopamine D1 receptors are supersensitive to dopamine receptor agonists because of the lack of dopamine tone (19), resulting in robust c-Fos induction after dopamine D1 receptor activation. vrDDfs mice treated with the dopamine D1 receptor agonist SKF-81297 had abundant c-Fos induction throughout the NAc, but not the CPu, compared with control mice, indicating that dopamine tone had been selectively restored to the CPu (see Fig. 8 *A–C*, which is published as supporting information on the PNAS web site).

Quantitative analyses of dopamine and dopamine metabolites were performed by HPLC-electrochemical detection and fast-scan cyclic voltammetry (FSCV). These techniques revealed that dopamine content was restored to ≈55% of control levels (see Table 1) and evoked release of dopamine to ≈30% of control levels (see Table 2, which is published as supporting information on the PNAS web site) in the CPu of vrDDfs mice. Dopamine levels were also elevated in the ventral striatum of vrDDfs but to a lesser extent. Evoked dopamine release was detectable in the ventral striatum but greatly reduced compared with the dorsal striatum, especially in the NAc.

Feeding Behavior. vrDDfs were no longer dependent on L-dopa for survival, and they rapidly gained BW after surgery (see Fig. 9, which is published as supporting information on the PNAS web site). They consumed significantly more laboratory chow than control mice over the course of 4 days (mean ± SEM: vrDDfs, 186 ± 14; control, 135 ± 15 mg/g BW per day) [repeated measures (rm)-ANOVA, genotype effect, $P < 0.01$]. To determine how the structure of feeding behavior was modified, vrDDfs and control mice were placed into lickometer cages with a highly palatable liquid diet. The experiment was separated into four phases: (*i*) animals were allowed to acclimate to the new diet and environment for 3 days, (*ii*) followed by 5 days of baseline acquisition, (*iii*) a 1-day fast, and (*iv*) 2 days of recovery (Fig. 3*A*). Whereas control mice showed a stable pattern of licking throughout the experiment, vrDDfs mice continued to increase their food intake over the course of the first few days (Fig. 3*A*). During the baseline phase, vrDDfs mice had a stable feeding pattern (Fig. 3*A*) and made significantly more licks than control mice (Fig. 3*B*). The amount of liquid diet consumed was also greater than control mice (Fig. 3*C*), demonstrating that the increase in licks made by vrDDfs mice represents increased consumption rather than a decreased lick efficiency. However, the number of meals (see *Methods* for meal definition) per day was not significantly greater in the vrDDfs mice (see Fig. 10*A*, which is published as supporting information on the PNAS web site). The discrepancy between the increased lick number, but not meal number, by vrDDfs mice can be explained by the increased consumption of very large meals as shown in Fig. 3*D* (meal size, mean ± SEM: vrDDfs, 612 ± 92; control, 435 ± 50 licks per meal). However, there were no significant changes in the distribution of meal durations (see Fig. 10*B*) (meal duration, mean ± SEM: vrDDfs, 139 ± 13; control, 129 ± 11 s per meal). Therefore, the large meal size is mostly because of the tendency of vrDDfs mice to lick at faster rates (Fig. 3*E*).

To determine to what extent the palatability of the liquid diet may contribute to the hyperphagia of vrDDfs mice, we examined the response to this diet in satiated mice. We limited availability of liquid diet to 2 h per day for 10 days with ad libitum access to standard chow during the remaining 22 h. The vrDDfs had greater consumption of liquid diet, as measured by total licks or volume consumed throughout the 10 days of the experiment (see Fig. 11, which is published as supporting information on the PNAS web site). Most of this difference occurred during the first 20 min, when vrDDfs made 2- to 4-fold more licks compared with controls (Fig. 4). Furthermore, after a 24-h fast, vrDDfs mice respond normally when solid, higher-fat breeder chow (5LJ5; 11% fat) is available (mean ± SEM: vrDDfs, 1.5 ± 0.2; control, 1.8 ± 0.2 grams per 4 h), but consume significantly less chow (5053; 4.5% fat) compared with control mice when the fat content is lower (mean ± SEM: vrDDfs, 0.7 ± 0.1; control, 1.6 ± 0.2 grams per 4 h; *t* test, $P < 0.01$).

Motor Behaviors. Although untreated DDfs mice were extremely hypoactive, after viral rescue they were hyperactive compared with control mice (Fig. 5*A*). They had a normal exploratory locomotor response (the first 6 h), but their nocturnal locomotor activity exceeded that of control mice (Fig. 5*A*). Hyperactivity was most variable during the first night in the locomotor chambers, so the second night of locomotion was analyzed

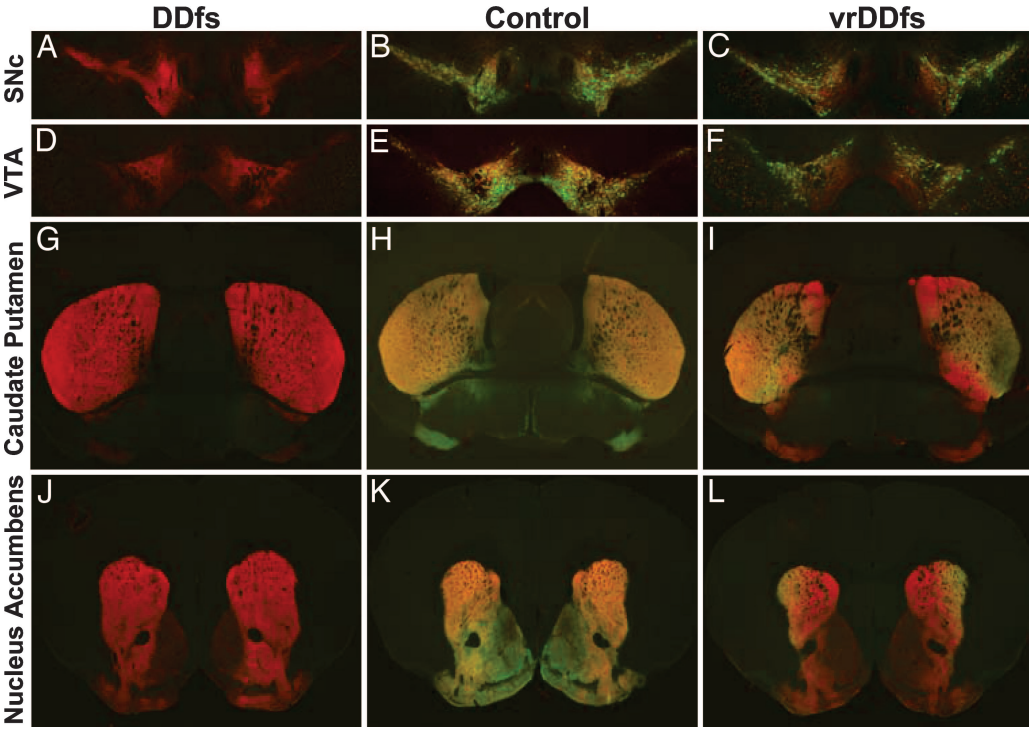

Fig. 2. *Th* (green) and dopamine transporter (red) immunostaining in coronal sections of brains from DDfs, control, and vrDDfs mice. (*A–F*) Sections through the SNc and VTA were subjected to immunohistochemistry with antisera to *Th* and DAT. There was no *Th* signal in DDfs mice, but DAT staining indicates the presence of intact dopamine neurons. *Th*+ neurons are abundant in the SNc of control and vrDDfs mice. There are a few *Th*+ cell bodies in the dorsal VTA of vrDDfs mice. (*G–L*) Sections through the striatum, showing projections of the midbrain dopamine neurons. *Th* staining was present throughout the CPu and ventrolateral striatum of vrDDfs mice. The medial shell and core of the NAc were devoid of *Th* signal in vrDDfs mice.

(nocturnal activity, mean ± SEM, $n = 24$ mice per genotype: vrDDfs, 5,326 ± 982; control, 2,519 ± 540 ambulations; t test, $P < 0.05$). Like DD mice (7, 8), L-dopa treatment stimulated locomotion in vrDDfs mice, whereas control mice were unresponsive (Fig. 5*B*). This locomotor induction is presumably because of the restoration of dopamine signaling to the ventral striatum.

To further characterize locomotor patterns, vrDDfs and control mice were videorecorded in the open field. The behavior of freely moving mice in the open field was analyzed by using SEE software (20). The SEE analysis of vrDDfs mice revealed a number of differences in behavior compared with control mice in the open field (see Table 3, which is published as supporting information on the PNAS web site). Many of these differences

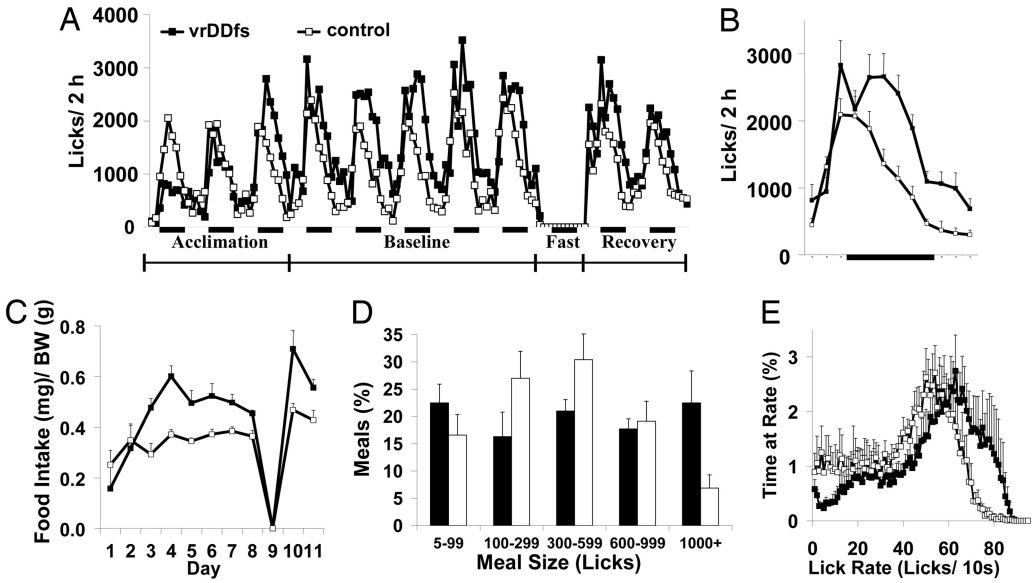

Fig. 3. Feeding behavior in lickometer cages by control ($n = 8$; open symbols) and vrDDfs ($n = 7$; filled symbols) mice on a novel, highly palatable liquid diet. (*A*) Lick time course in 2-h bins over 11 days (white bars) and nights (dark bars). The experiment is separated into four phases as shown. vrDDfs mice required more time to achieve a steady-state baseline feeding pattern (rm-ANOVA on acclimation days 1 to 3, genotype × time interaction, $P < 0.001$; rm-ANOVA on days 4–8, genotype effect $P < 0.01$). (*B*) Average baseline licking was significantly greater for vrDDfs mice over the 24-h feeding cycle (rm-ANOVA, genotype effect $P < 0.05$, genotype × time interaction, $P < 0.001$). (*C*) Food intake (by weight) was also greater in vrDDfs mice, demonstrating that the increased licking does not simply reflect decreased lick efficiency (rm-ANOVA on days 4–8, genotype effect $P < 0.01$). (*D*) The distribution of meal sizes during the baseline phase is different in vrDDfs mice compared with controls (rm-ANOVA, genotype × size interaction, $P < 0.05$) with the largest difference being the increase in very large meals (>1,000 licks) in vrDDfs mice. (*E*) The distribution of lick rates during baseline phase meals is shifted in vrDDfs mice, indicating that they spend more time licking at faster rates (rm-ANOVA, genotype × rate interaction $P < 0.001$). All data expressed as means ± SEM.

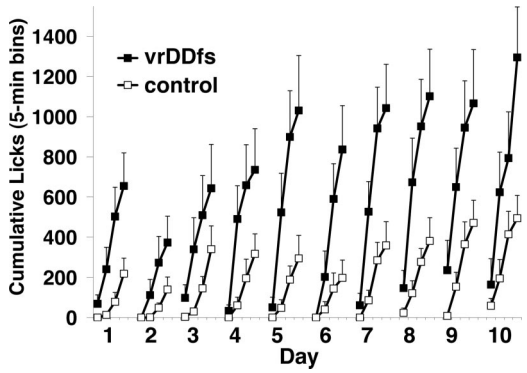

Fig. 4. Lickometer analysis of fed control ($n = 8$) and vrDDfs ($n = 8$) mice with 2 h of access to highly palatable liquid diet for 10 consecutive days. Both genotypes increased consumption of liquid diet over the course of 10 days, but the vrDDfs mice had more licks per day and a steeper rate of increase; most of this increase occurred during the first 20 min (shown here) of access to the diet (rm-ANOVA, genotype effect $P < 0.05$, day effect $P < 0.001$, genotype $\times$ day interaction $P < 0.05$). All data expressed as means $\pm$ SEM.

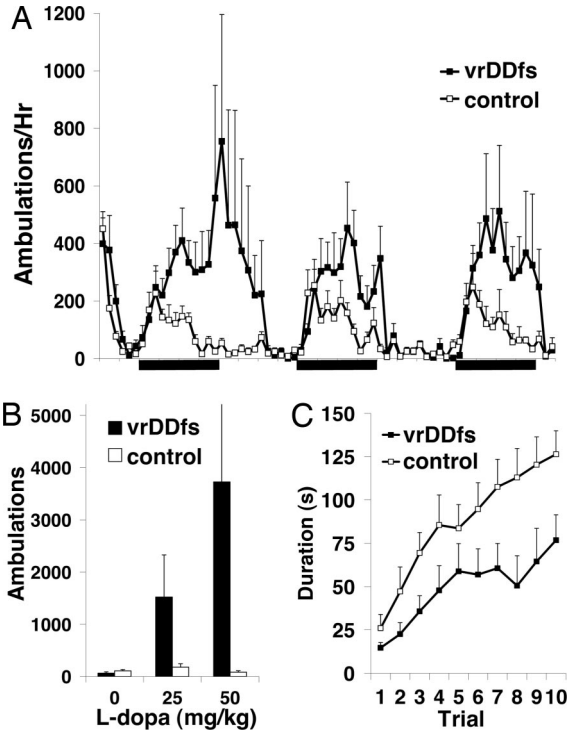

Fig. 5. Locomotor activity of control ($n = 8$) and vrDDfs ($n = 8$) mice. (*A*) Representative 3-day locomotor time course. vrDDfs mice are hyperactive relative to control mice during the nocturnal phase (dark bars). (*B*) L-dopa induces a dose-dependent locomotor response in vrDDfs but not control mice (rm-ANOVA, treatment effect $P < 0.05$, genotype $\times$ treatment interaction $P < 0.05$). (*C*) Rotarod performance improved over ten trials in both genotypes but was impaired in the vrDDfs mice compared with control mice (rm-ANOVA, genotype effect $P < 0.05$, trial effect $P < 0.001$). All data expressed as means $\pm$ SEM.

were related to their activity in the center of the open field. Indeed, the vrDDfs mice stayed closer to the wall compared with controls (distance from wall, mean $\pm$ SEM: vrDDfs, 5.5 $\pm$ 0.5; control, 8.0 $\pm$ 0.5 cm; *t* test, $P < 0.01$). Because thigmotactic behavior can be indicative of increased levels of anxiety (21), we tested the mice on the elevated-plus maze. Although the vrDDfs mice displayed a tendency to spend less time in, and make fewer entries into, the open arms of the maze, none of the differences were significant (see Fig. 12, which is published as supporting information on the PNAS web site).

We also tested the mice on the rotarod to examine their ability to perform and learn a complex motor task. The vrDDfs mice performed the task and improved with practice, but their performance was significantly worse than control mice over the course of ten trials (Fig. 5*C*).

Discussion

We describe a strategy that uses a Th^{fs} allele and a retrogradely transported viral vector to restore dopamine in a circuit-selective manner. This strategy offers several advantages over previous viral-based approaches and lesion models. The efficient retrograde transport of the CAV-2 vector (15, 16) makes it well-suited for expressing genes in neurons that project to specific target fields. By using this vector to express Cre recombinase, we activated the endogenous *Th* gene and thus achieved *Th* expression only in those cells that normally express this gene. Selective restoration of dopamine signaling to specific dopaminergic neurons in DDfs mice can be used to address some of the same questions that have classically been addressed by using neurotoxins like 6-hydroxydopamine; however, our method is inherently more specific in that only one neurotransmitter is affected. Recent observations suggesting that dopamine neurons corelease glutamate (22, 23) highlight the relevance of this point.

Our results showing that vrDDfs mice had restored locomotor activity, as well as food intake, are surprising in light of our previous work using adeno-associated viruses (AAV) to restore dopamine production to the striatum. In previous experiments, the mice that had dopamine restored to the CPu ate sufficiently to survive, but they remained relatively hypoactive; in contrast, the mice with dopamine restored to the NAc had a relatively normal locomotor response to novelty, but they did not feed adequately (12). Another distinction between the models is that adequate feeding could not be restored via unilateral AAV delivery (13), despite the fact that unilateral 6-hydroxydopamine lesions do not abolish feeding. In contrast, by using the current model, we achieved unilateral rescue of feeding behavior in most (14 of 19) attempts (data not shown). These differences may reflect the ability of CAVCre to restore *Th* much more widely throughout the CPu rather than to a small area around the site of injection. This widespread expression of *Th* throughout the CPu by using the CAVCre method indicates that at least some of the dopamine neurons in which the endogenous *Th* gene is activated have extensive arborization that encompass large portions of the CPu (2, 24). The dopamine content in tissue punches from the CPu of vrDDfs mice was $\approx$2-fold higher than DD mice rescued with AAV (12). Another important distinction between the two viral approaches is that CAVCre restores *Th* synthesis directly to the dopamine neurons, as opposed to inducing L-dopa production in nondopaminergic striatal cells at the site of injection. Consequently, somato-dendritic release of dopamine and autoreceptor-mediated inhibition of midbrain dopamine neurons should be restored in this model. Additionally, CAVCre restores transcription of the endogenous *Th* gene rather than relying on a viral promoter to drive *Th* gene expression; thus, *Th* gene regulation should be normal.

Alternatively, the more complete behavioral rescue of the vrDDfs mice may be because of production and release of dopamine outside of the CPu. We observed some *Th*-positive cell bodies in the dorsal VTA, indicating that some VTA neurons send projections or collaterals to the CPu; we also observed fiber staining in lateral regions of the ventral striatum and low levels of dopamine in the NAc. Although dopamine levels in the NAc were low, medium spiny neurons can compensate by increasing their responsiveness to dopamine (19). Thus, even a small amount of dopamine in the NAc may have behaviorally signif-

icant effects. However, the robust induction of c-Fos by the dopamine D1 receptor agonist in the NAc suggests that dopamine tone is lacking. Moreover, the dopamine metabolite 3-methoxytyramine was undetectable in the NAc of 6/6 vrDDfs mice (see Table 1). Catechol-0-methyltransferase metabolizes extracellular dopamine into 3-methoxytyramine; thus, its production is often used as a marker for dopamine release (25). This result suggests that, although evoked dopamine can be detected in the NAc *in vitro*, its extracellular concentration under basal conditions is insignificant.

The bradykinesia and hypoactivity of DDfs mice is dramatically reversed in the vrDDfs mice. Daytime exploratory responses of vrDDfs mice are similar to control mice, and their nocturnal activity exceeds that of control mice, although they still manifest a deficit in rotarod performance throughout 10 days of training. The nocturnal hyperactivity is consistent with results where 6-hydroxydopamine was used to specifically lesion the VTA (26, 27). Thus, these observations may reflect a deficiency or a functional imbalance of dopamine signaling within the striatum because of the relative lack of dopamine in the ventral compared with the dorsal striatum. Another explanation for the nocturnal hyperactivity is that the increased dopamine release that occurs at night (28, 29) increases diffusion of dopamine farther from the release site, where it may activate dopamine receptors on hypersensitive cells (19).

Before viral rescue, the DDfs mice are lean. Hence, the initial hyperphagia by vrDDfs mice may reflect a metabolic drive to achieve normal BW. However, vrDDfs mice continue to consume more food after they reach the BW of control littermates. Perhaps the increased nocturnal activity drives an increase in food consumption to compensate for the increased energy demand or vice versa. It is also interesting that the hyperphagia manifests as an increased lick rate rather than more or longer meals. The increased lick rate could imply a role for dopamine in the regulation of the orosensory effects of the liquid diet on licking (30). For instance, the vrDDfs mice may lick faster because of enhanced perception of palatability, a conclusion supported by our finding that satiated vrDDfs mice begin consuming the liquid diet more rapidly than control mice.

Another possibility is that the absence of dopamine during early development (before day 10) or daily treatment with L-dopa (from day 10 until viral rescue) led to compensatory changes that mediate hyperactivity and hyperphagia. However, the absence of such phenotypes in our previous viral rescue approaches argues against this interpretation (12, 13).

The alterations in feeding behavior are likely a result of the absence of dopamine signaling in brain regions outside of the CPu (e.g., NAc or hypothalamus), where dopamine signaling has been shown to influence feeding. For instance, the NAc has a modulatory role in food intake, especially of highly palatable diets (5). Blocking either opioid or α-amino-3-hydroxy-5-methyl-4-isoxazolepropionic acid (AMPA) receptors in the NAc disinhibits signaling to the hypothalamus and stimulates feeding (31–34). Furthermore, dopamine levels in the hypothalamus increase during meal onset and hypothalamic dopamine signaling can influence food intake (35, 36). In addition, hypothalamic tuberoinfundibular dopamine neurons regulate pituitary function (37), and pituitary hormones such as prolactin (38, 39), growth hormone (39), or adrenocorticotropic hormone (40) may affect food consumption and/or preferences. Absence of dopamine in any of these brain regions may contribute to hyperphagia and/or increased meal sizes by vrDDfs mice.

Although we described several important differences between the vrDDfs and control mice, it is remarkable that restoration of *Th* production selectively to neurons that project to the CPu dramatically reverses the bradykinesia and hypophagia phenotypes that characterize DDfs (and DD) mice. Unlike the DDfs mice, which are largely unresponsive to external stimuli, the vrDDfs mice are able to perform every task examined, although the magnitude of their responses vary compared with control mice. Our results support the hypothesis that dopamine signaling in the CPu is sufficient to energize most (if not all) goal-directed behaviors. However, more challenging tasks may reveal behaviors dependent on dopamine outside of the CPu (41).

Methods

Generation of vrDDfs Mice. $Th^{fs/+}$ mice were generated by gene targeting. Similar to the breeding strategy used in ref. 7, we generated DDfs ($Th^{fs/fs}$; $Dbh^{Th/+}$) mice carrying two conditionally inactive *Th* alleles, one intact *Dbh* allele (Dbh^{+}), and one *Dbh* allele with a targeted insertion of the *Th* gene (Dbh^{Th}). Control animals carry at least one intact *Th* allele and one intact *Dbh* allele (see Fig. 6) and synthesize normal levels of catecholamines. Mice were maintained on a mixed C57BL/6X 129S4 genetic background. All mice were housed under a 12:12 light:dark cycle in a temperature-controlled environment with food (5LJ5; PMI Feeds, St. Louis) and water available ad libitum unless noted. All mice were treated in accordance with guidelines established by the National Institutes of Health and the University of Washington Animal Care Committee.

Recombinant CAV-2 vectors engineered to express CAVCre driven by the cytomegalovirus promoter were generated and titered as described (14). The vector preparation had a titer of 6×10^{12} physical particles per ml. Bilateral injections of 0.5–0.55 μl CAVCre into the central region of the CPu (coordinates in mm: +0.80 anterior to Bregma, +2.00 and −2.00 lateral to midline; 3.60 ventral to skull surface) were performed on anesthetized (ketamine, xylazine, acepromazine) 3- to 5-month-old DDfs and control mice (mixed sex) as described (12, 13, 17, 18). DDfs mice were removed from L-dopa treatment ≈1 week after viral injection, and those mice that maintained BW after 1 week without L-dopa treatment were designated as virally rescued (i.e., vrDDfs). Of >100 mice that have been treated this way, ≈95% were rescued.

Behavioral Studies. To measure feeding, vrDDfs and control littermates (4–6 weeks after viral injection) were placed into lickometer chambers (Columbus Instruments, Columbus, OH), which were used as described (42). Mice had access to liquid diet (5LD-101; PMI Feeds) and water throughout the experiment unless specified. On the first day of acclimation (day 1), they also had access to their standard laboratory chow (5LJ5), which was removed after 24 h. Much of the data reported here were analyzed from feeding during the baseline phase because mice of both genotypes were licking in stable patterns. Each day, the BW and amount of liquid diet consumed were measured. Events (licks) were collected by the program Event Counter (Columbus Instruments) in 10-s bins, which were analyzed in 2-h bins by software of our own design based on PYTHON code. Meals were defined as any number of consecutive 10-s bins in which an animal made at least 5 licks separated by 12 or more 10-s bins (i.e., 2 min) without licks (10-s bins that contained ≤4 licks, which were not within a meal, were defined as zero, because they are likely to be spurious events). These parameters were chosen because they allow for the inclusion of nearly all of the licks into meals, however, data were analyzed with multiple meal definitions which varied the minimum number of licks per meal and the minimum time necessary between meals; all conditions examined produced qualitatively similar results. In a separate experiment, naïve groups of mice were preexposed to the liquid diet (LD 101) for 48 h in their home cages. Five days later, they were placed into lickometer chambers for 2 h where they had access to the liquid diet. For the remaining 22 h, the mice were returned to their home cages with access to their standard laboratory chow (5LJ5). This feeding schedule was repeated for 10 consecutive days.

Locomotion was measured by using photobeam-equipped activity chambers as described (19). An ambulation is scored each time an animal breaks two consecutive photobeams. In the dose-response experiment, mice were treated with increasing doses of L-dopa (0, 25, 50, mg/kg i.p.; Sigma Aldrich) once per day over the course of 3 consecutive days, and activity was recorded for 6 h. Rotarod (Rotamex 4/8 system; Columbus Instruments) analysis was performed over 5 consecutive days with two trials per day. Mice were placed on the rotarod, which began at 4 rpm and accelerated to 40 rpm over the course of 5 min; the latency to fall was recorded.

Immunohistochemistry and Quantification of Dopamine. Anesthetized mice were perfused transcardially with PBS, followed by 4% paraformaldehyde (PFA) in PBS. Brains were dissected, postfixed in PFA overnight, cryoprotected in 30% sucrose, and frozen. Free-floating coronal sections (30 to 40 μm) were immunostained by using one or more of the following primary antibodies: rabbit anti-TH (1:2000; Chemicon), rat anti-dopamine transporter (DAT) (1:1000, Chemicon), and/or goat anti-c-Fos (1:5,000; Santa Cruz Biotechnology). Immunofluorescence was revealed by using CY2 and/or CY3 labeled IgG secondary antibodies (1:200; Jackson ImmunoResearch). Sections were mounted on slides, coverslips were applied, and the sections were photographed.

HPLC coupled with electrochemical detection was used to measure monoamine content by the Neurochemistry Core Laboratory at Vanderbilt University's Center for Molecular Neuroscience Research (43). Voltammetric measurement of electrically evoked dopamine release was performed on 400-μm thick coronal sections. For more details, see Tables 1 and 2.

We thank Glenda Froelick for histological assistance, Bethany Sotak and Nora Meneses for colony maintenance, Colin Phillips for help with data collection, Victor Denenberg for statistical advice, and David Perkel for use of equipment. We thank the National Institute on Drug Abuse (NIDA) Center at the University of Washington for use of behavioral equipment, space, and software. E.J.K. is Directeur de Recherche at Institut National de la Santé et de la Recherche Médicale and is supported by the Association Francaise Contre les Myopathies and Vaincre Les Maladies Lysosomales. T.S.H. was supported in part by National Institute of General Medical Sciences Grant PHS NRSA T32 GM07270.

1. German, D. C., Schlusselberg, D. S. & Woodward, D. J. (1983) *J. Neural. Transm.* **57,** 243–254.
2. Björkland, A. & Lindvall, O. (1984) in *Classical Transmitters in the CNS,* Handbook of Chemical Neuroanatomy, eds. Björkland, A. & Hökfelt, T. (Elsevier, Amsterdam), Vol. 2, part 1, pp. 55–122.
3. Berridge, K. C. & Robinson, T. E. (1998) *Brain Res. Brain Res. Rev.* **28,** 309–369.
4. Schultz, W. (2006) *Annu. Rev. Psychol.* **57,** 87–115.
5. Kelley, A. E., Baldo, B. A. & Pratt, W. E. (2005) *J. Comp. Neurol.* **493,** 72–85.
6. Wise, R. A. (2004) *Nat. Rev. Neurosci.* **5,** 483–494.
7. Zhou, Q. Y. & Palmiter, R. D. (1995) *Cell* **83,** 1197–1209.
8. Szczypka, M. S., Rainey, M. A., Kim, D. S., Alaynick, W. A., Marck, B. T., Matsumoto, A. M. & Palmiter, R. D. (1999) *Proc. Natl. Acad. Sci. USA* **96,** 12138–12143.
9. Denenberg, V. H., Kim, D. S. & Palmiter, R. D. (2004) *Behav. Brain Res.* **148,** 73–78.
10. Hnasko, T. S., Sotak, B. N. & Palmiter, R. D. (2005) *Nature* **438,** 854–857.
11. Robinson, S., Sandstrom, S. M., Denenberg, V. H. & Palmiter, R. D. (2005) *Behav. Neurosci.* **119,** 5–15.
12. Szczypka, M. S., Kwok, K., Brot, M. D., Marck, B. T., Matsumoto, A. M., Donahue, B. A. & Palmiter, R. D. (2001) *Neuron* **30,** 819–828.
13. Szczypka, M. S., Mandel, R. J., Donahue, B. A., Snyder, R. O., Leff, S. E. & Palmiter, R. D. (1999) *Neuron* **22,** 167–178.
14. Kremer, E. J., Boutin, S., Chillon, M. & Danos, O. (2000) *J. Virol.* **74,** 505–512.
15. Soudais, C., Skander, N. & Kremer, E. J. (2004) *FASEB J.* **18,** 391–393.
16. Soudais, C., Laplace-Builhe, C., Kissa, K. & Kremer, E. J. (2001) *FASEB J.* **15,** 2283–2285.
17. Sotak, B. N., Hnasko, T. S., Robinson, S., Kremer, E. J. & Palmiter, R. D. (2005) *Brain Res.* **1061,** 88–96.
18. Hnasko, T. S., Szczypka, M. S., Alaynick, W. A., During, M. J. & Palmiter, R. D. (2004) *Brain Res.* **1023,** 309–318.
19. Kim, D. S., Szczypka, M. S. & Palmiter, R. D. (2000) *J. Neurosci.* **20,** 4405–4413.
20. Drai, D. & Golani, I. (2001) *Neurosci. Biobehav. Rev.* **25,** 409–426.
21. Simon, P., Dupuis, R. & Costentin, J. (1994) *Behav. Brain Res.* **61,** 59–64.
22. Chuhma, N., Zhang, H., Masson, J., Zhuang, X., Sulzer, D., Hen, R. & Rayport, S. (2004) *J. Neurosci.* **24,** 972–981.
23. Lavin, A., Nogueira, L., Lapish, C. C., Wightman, R. M., Phillips, P. E. & Seamans, J. K. (2005) *J. Neurosci.* **25,** 5013–5023.
24. Fallon, J. H. & Loughlin, S. E. (1982) *Brain Res. Bull.* **9,** 295–307.
25. Wood, P. L. & Altar, C. A. (1988) *Pharmacol. Rev.* **40,** 163–187.
26. Koob, G. F., Stinus, L. & Le Moal, M. (1981) *Behav. Brain Res.* **3,** 341–359.
27. Oades, R. D., Taghzouti, K., Rivet, J. M., Simon, H. & Le Moal, M. (1986) *Neuropsychobiology* **16,** 37–42.
28. Paulson, P. E. & Robinson, T. E. (1994) *Behav. Neurosci.* **108,** 624–635.
29. Smith, A. D., Olson, R. J. & Justice, J. B. (1992) *J. Neurosci. Methods* **44,** 33–41.
30. Schneider, L. H., Davis, J. D., Watson, C. A. & Smith, G. P. (1990) *Eur. J. Pharmacol.* **186,** 61–70.
31. Kelley, A. E. & Swanson, C. J. (1997) *Behav. Brain Res.* **89,** 107–113.
32. Will, M. J., Franzblau, E. B. & Kelley, A. E. (2003) *J. Neurosci.* **23,** 2882–2888.
33. Zhang, M., Gosnell, B. A. & Kelley, A. E. (1998) *J. Pharmacol. Exp. Ther.* **285,** 908–914.
34. Zhang, M., Balmadrid, C. & Kelley, A. E. (2003) *Behav. Neurosci.* **117,** 202–211.
35. Leibowitz, S. F. & Rossakis, C. (1978) *Eur. J. Pharmacol.* **53,** 69–81.
36. Meguid, M. M., Fetissov, S. O., Varma, M., Sato, T., Zhang, L., Laviano, A. & Rossi-Fanelli, F. (2000) *Nutrition* **16,** 843–857.
37. Ben Jonathan, N. & Hnasko, R. (2001) *Endocr. Rev.* **22,** 724–763.
38. Gerardo-Gettens, T., Moore, B. J., Stern, J. S. & Horwitz, B. A. (1989) *Am. J. Physiol.* **256,** R276–R280.
39. Byatt, J. C., Staten, N. R., Salsgiver, W. J., Kostelc, J. G. & Collier, R. J. (1993) *Am. J. Physiol.* **264,** E986–E992.
40. Dallman, M. F., Pecoraro, N., Akana, S. F., La Fleur, S. E., Gomez, F., Houshyar, H., Bell, M. E., Bhatnagar, S., Laugero, K. D. & Manalo, S. (2003) *Proc. Natl. Acad. Sci. USA* **100,** 11696–11701.
41. Salamone, J. D., Correa, M., Mingote, S. M., Weber S. M. (2005) *Curr. Opin. Pharmacol.* **5,** 34–41.
42. Cannon, C. M. & Palmiter, R. D. (2003) *J. Neurosci.* **23,** 10827–10831.
43. Perez, F. A. & Palmiter, R. D. (2005) *Proc. Natl. Acad. Sci. USA* **102,** 2174–2179.

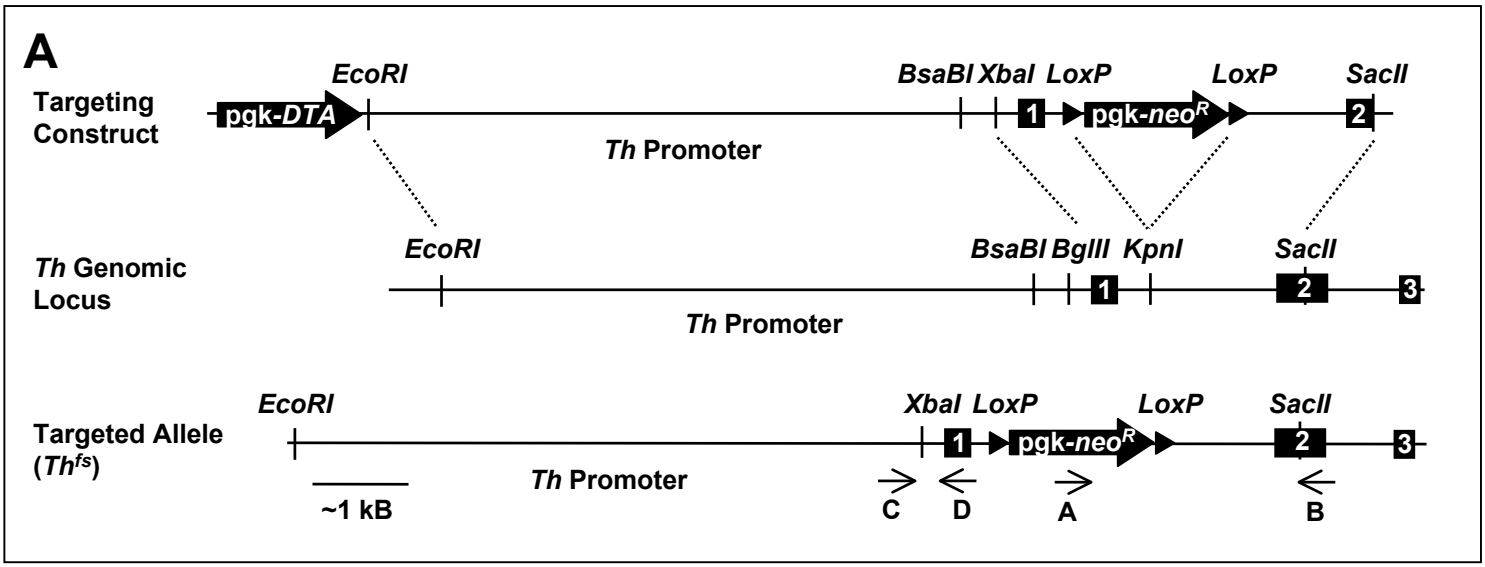

B

$Th^{fs/+}, Dbh^{Th/+}$ x $Th^{fs/+}, Dbh^{Th/+}$

- $Th^{fs/fs}, Dbh^{Th/+}$ (DDfs)
- controls:
  - $Th^{fs/+}, Dbh^{Th/+}$
  - $Th^{fs/+}, Dbh^{+/+}$
  - $Th^{+/+}, Dbh^{Th/+}$
  - $Th^{+/+}, Dbh^{+/+}$
- lethal:
  - $Th^{fs/+}, Dbh^{Th/Th}$
  - $Th^{+/+}, Dbh^{Th/Th}$
  - $Th^{fs/fs}, Dbh^{Th/+}$
  - $Th^{fs/fs}, Dbh^{+/+}$

Table 3. SEE analysis of open-field behavior

	Endpoint	vrDDfs	Control	*P*
*	DistanceTraveled (cm)	5614 +/- 831	7815 +/- 438	0.0260
	LingeringMeanSpeed (s)	1.42 +/- 0.17	1.39 +/- 0.08	0.8603
***	ProportionOfTimeSpentAwayFromWall	0.329 +/- 0.047	0.566 +/- 0.036	0.0004
**	ProportionOfLingeringTimeAwayFromWall	0.208 +/- 0.030	0.341 +/- 0.028	0.0028
***	ProportionOfLingeringTimeAwayFromWall2	0.298 +/- 0.048	0.523 +/- 0.037	0.0008
	NumberOfProgressionSegments	209 +/- 20	247 +/- 13	0.1276
	MedianSpatialSpreadOfLingeringEpisodes (cm)	1.26 +/- 0.11	1.22 +/- 0.10	0.8193
*	MedianLengthOfProgressionSegments (cm)	16.2 +/- 2.0	22.1 +/- 1.2	0.0167
	MedianDurationOfLingeringEpisodes (s)	1.48 +/- 0.16	1.40 +/- 0.07	0.6163
	Quantile5ofDurationOfProgressionSegments (s)	0.446 +/- 0.044	0.503 +/- 0.025	0.2715
	Quantile95ofDurationOfProgressionSegments (s)	3.14 +/- 0.25	3.67 +/- 0.096	0.0553
	MedianDurationOfProgressionSegments (s)	1.22 +/- 0.11	1.44 +/- 0.047	0.0709
**	Quantile95OfMoveSegmentMaxSpeed (cm/s)	27.9 +/- 2.5	37.3 +/- 1.390	0.0028
*	MedianOfMoveSegmentMaxSpeed (cm/s)	17.7 +/- 1.9	23.2 +/- 1.018	0.0161
	MedianOfLingeringSegmentMaxSpeed (cm/s)	2.39 +/- 0.35	1.96 +/- 0.369	0.4042
	MedianSegmentAccelerationToMaxSpeed (cm/s^2)	14.9 +/- 0.7	16.1 +/- 0.606	0.1848
	Dart	1.085 +/- 0.077	1.071 +/- 0.027	0.8627
	MedianTurnRate (degrees/s)	14.8 +/- 1.0	14.0 +/- 0.397	0.4704
*	MedianRadiusOfTurn (cm)	62.8 +/- 5.5	76.6 +/- 2.810	0.0328
	LatencyToMaxHalfSpeed (s)	69.1 +/- 26.9	54.6 +/- 15.869	0.6447
	Diversity (cm)	46.7 +/- 3.2	50.3 +/- 1.096	0.2886
***	CenterActivityProportion	0.445 +/- 0.038	0.682 +/- 0.032	0.0001
**	CenterRestProportion	0.364 +/- 0.046	0.529 +/- 0.033	0.0068
*	TimeProportionOfLingeringEpisodes	0.749 +/- 0.031	0.653 +/- 0.018	0.0119
**	ActivityProportionOfLingeringEpisodes	0.272 +/- 0.039	0.141 +/- 0.008	0.0028
	MaxSpatialSpreadOfLingeringSegments (cm)	30.2 +/- 5.2	21.2 +/- 1.413	0.1049
*	MaxSpatialSpreadOfMoveSegments (cm)	70.8 +/- 6.4	87.4 +/- 1.405	0.0166
	ProportionOfRestingAtHomeBase	0.288 +/- 0.047	0.186 +/- 0.030	0.0745
	NumberOfStopsPerDistance (segments/cm)	0.064 +/- 0.020	0.032 +/- 0.001	0.1291
	NumberOfExcursions	12.8 +/- 1.9	17.1 +/- 1.479	0.0879
	NumberOfStopsPerExcursion	15.4 +/- 2.1	12.4 +/- 1.025	0.2137
	LingeringProgressionThresholdSpeed (cm/sec)	10.6 +/- 1.0	11.8 +/- 0.531	0.3047
**	HomeBaseRelativeOccupancy (degrees)	0.409 +/- 0.054	0.245 +/- 0.024	0.0095
	RelativeActivityDecrease	0.98 +/- 0.15	0.90 +/- 0.043	0.6373
	MedianCurvatureOfProgressionSegments	-0.067 +/- 0.073	0.011 +/- 0.040	0.3536
	MedianCurvatureOfWallSegments	-0.398 +/- 0.321	0.029 +/- 0.055	0.1998
	MedianCurvatureOfCenterSegments	0.018 +/- 0.069	-0.002 +/- 0.043	0.8066

Behavioral analysis of control (*n*=16) and vrDDfs (*n*=16) mice in the open field using Software for the Exploration for Exploration (SEE, www.tau.ac.il/~ilan99/see/SEEgeneral.htm). The open-field test consisted of placing a mouse near the perimeter of a circular 1-meter novel environment and allowing it to explore for 20 min while videotaping. ETHOVISION (Noldus) software was used for tracking. The x-y coordinates of the animal were entered into SEE. A wall/center radius of 5 cm was used for additional analysis. The values are means ± SEM with *P* values (*t* tests) for each measure (∗, $P < 0.05$; ∗∗, $P < 0.01$; ∗∗∗, $P < 0.001$ vrDDfs *vs* WT). However, signifigance should be interpreted cautiously because multiple *t* tests were performed and because some of these data do not fit normal distributions.

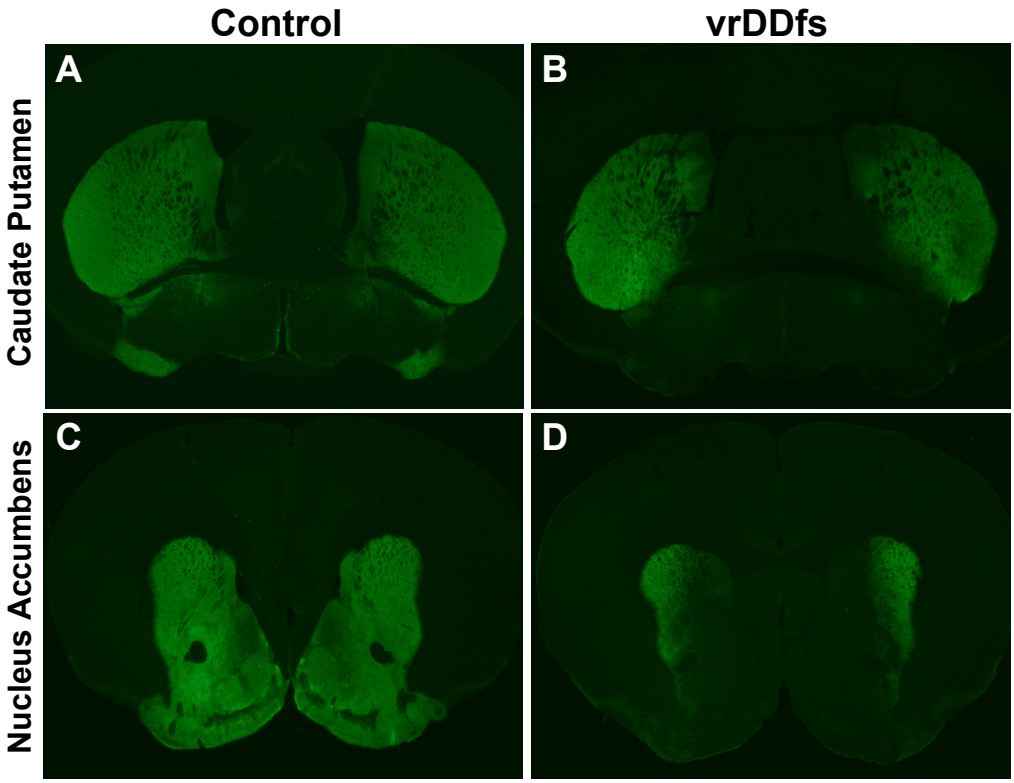
Control
vrDDfs
A
B
C
D
Caudate Putamen
Nucleus Accumbens

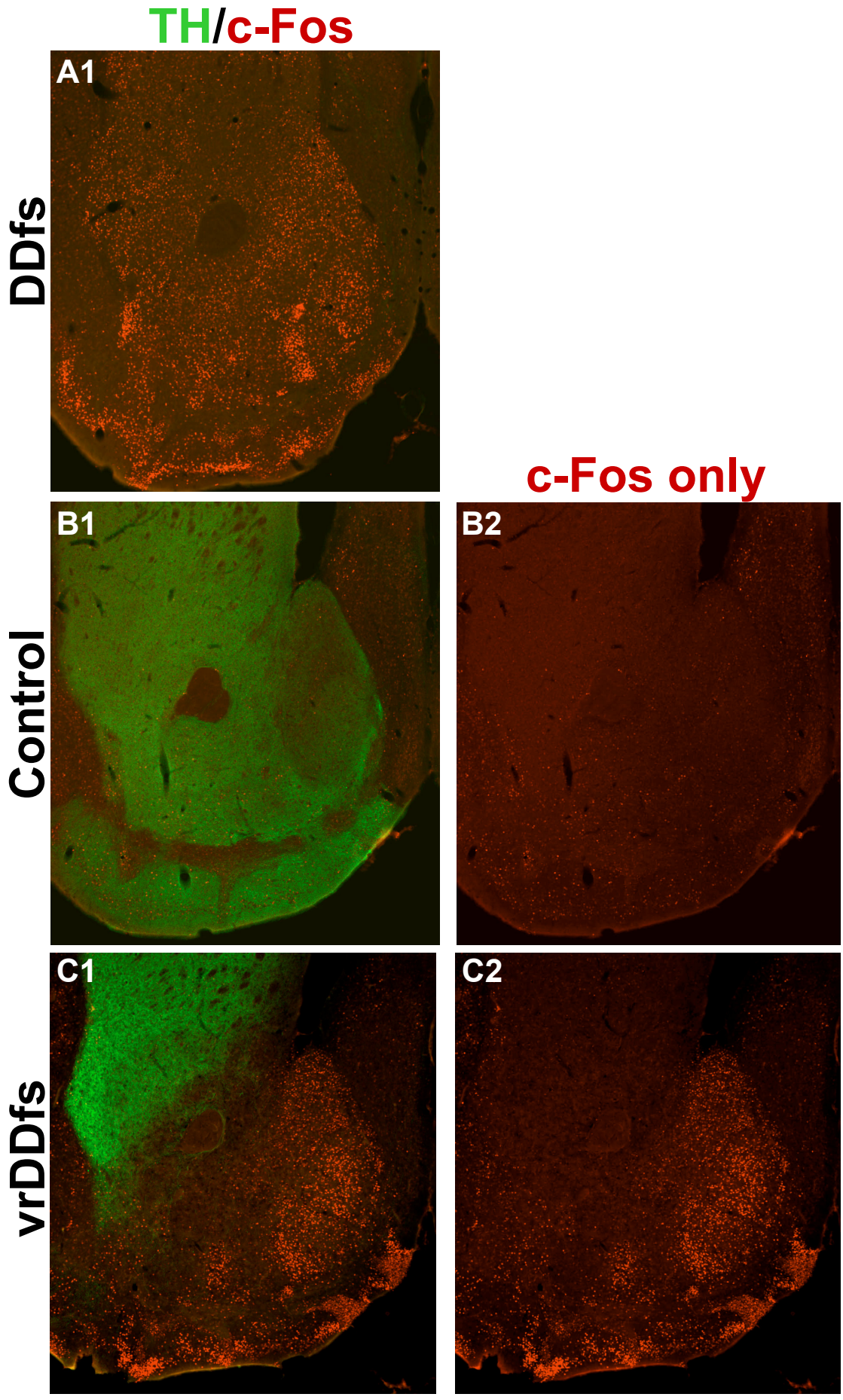
TH/c-Fos
c-Fos only
DDfs
Control
vrDDfs
A1
B1
B2
C1
C2

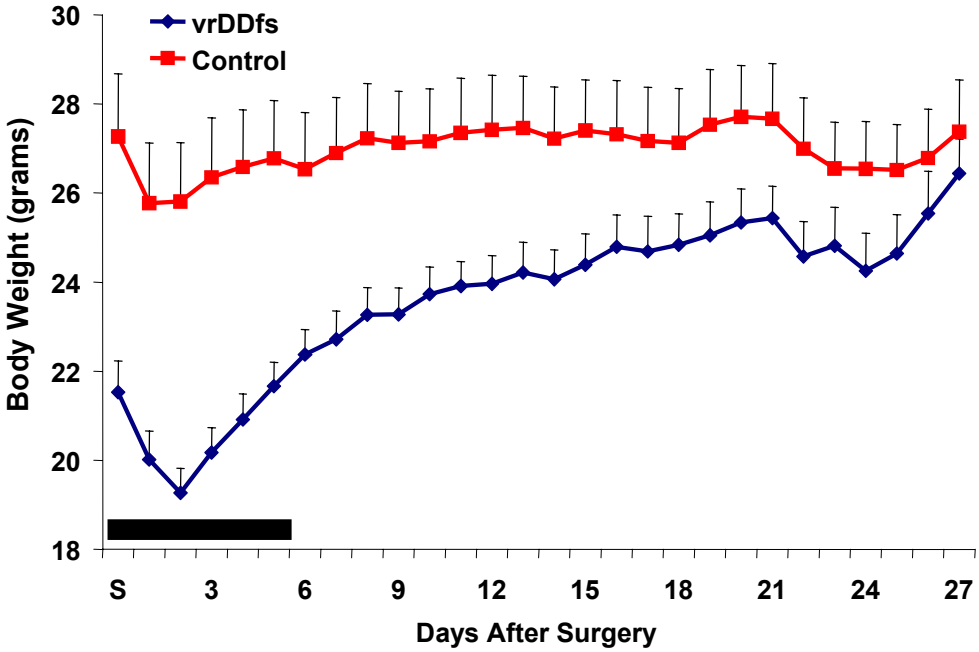
vrDDfs
Control
Body Weight (grams)
30
28
26
24
22
20
18
S
3
6
9
12
15
18
21
24
27
Days After Surgery

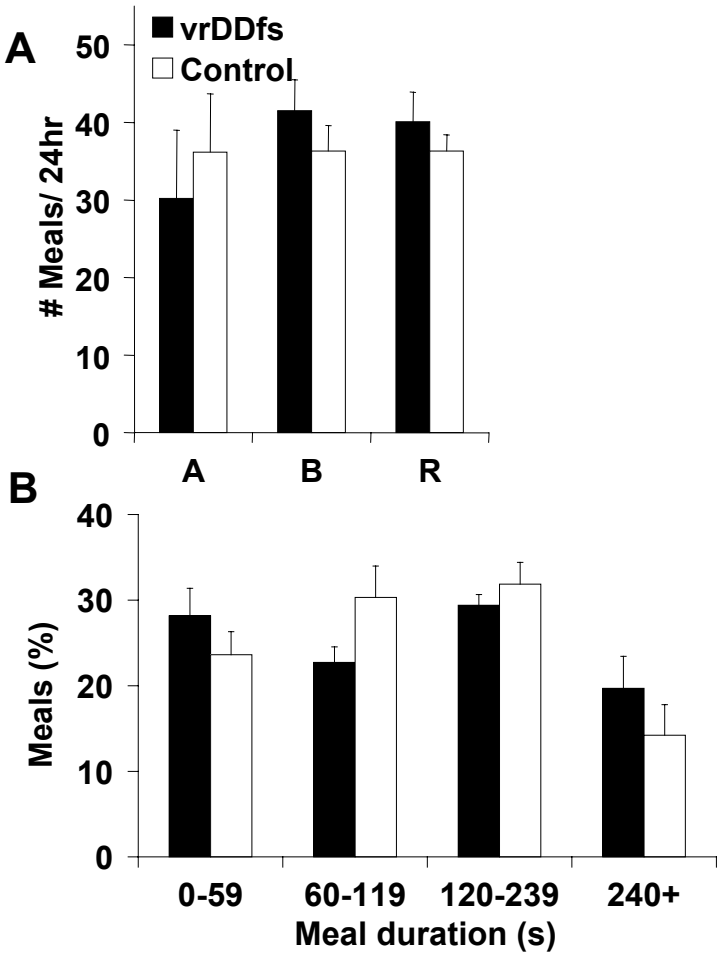
A
vrDDfs
Control
Meals/ 24hr
50
40
30
20
10
0
A
B
R
B
Meals (%)
40
30
20
10
0
0-59
60-119
120-239
240+
Meal duration (s)

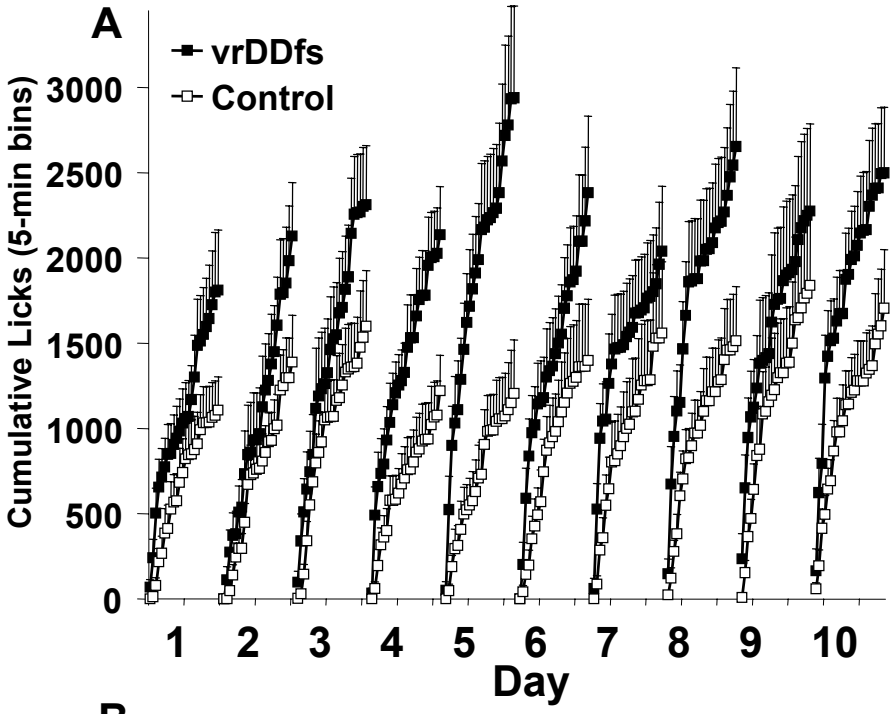
A
vrDDfs
Control
Cumulative Licks (5-min bins)
3000
2500
2000
1500
1000
500
0
1
2
3
4
5
6
7
8
9
10
Day

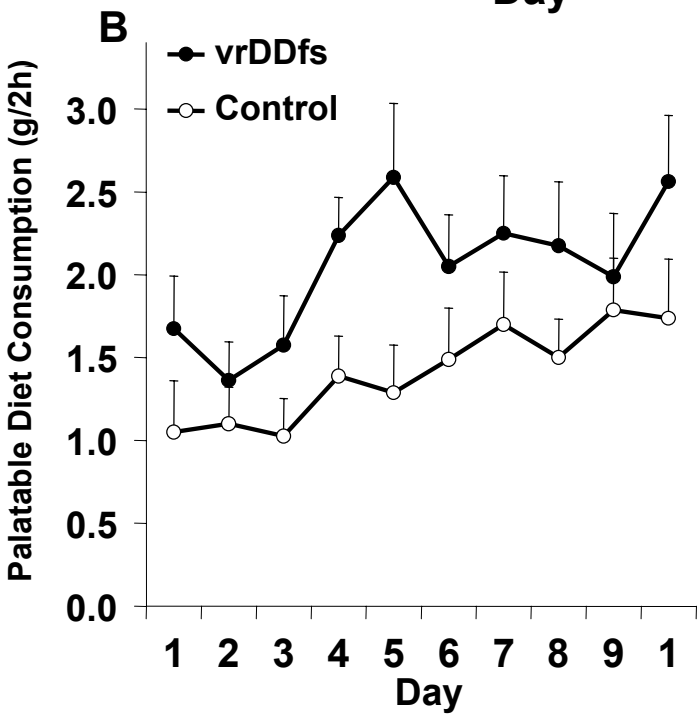
B
vrDDfs
Control
Palatable Diet Consumption (g/2h)
3.0
2.5
2.0
1.5
1.0
0.5
0.0
1
2
3
4
5
6
7
8
9
1
Day

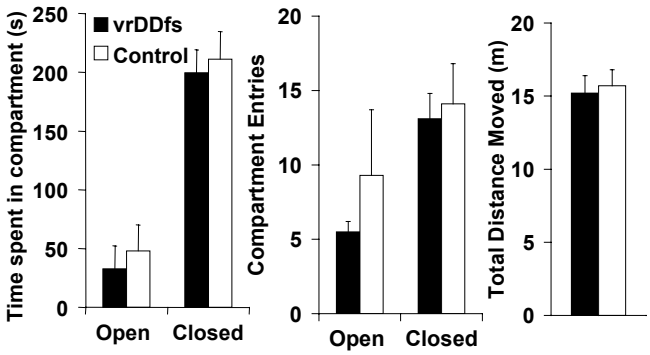
Time spent in compartment (s)
250
200
150
100
50
0
vrDDfs
Control
Open
Closed
Compartment Entries
20
15
10
5
0
Open
Closed
Total Distance Moved (m)
20
15
10
5
0

Table 1. HPLC quantification of dopamine and metabolite levels

Group	*n*	Region	DA (% Control)	DA (ng/mg)	HVA (ng/mg)	DOPAC (ng/mg)	3-MT(ng/mg)
DDfs	4	CPu	0.56	0.69 ± 0.04	0.99 ± 0.83	0.21 ± 0.07	n.d.
vrDDfs	6	CPu	56.2	69.1 ± 10.7	4.90 ± 0.69	3.39 ± 0.50	6.72 ± 0.68
Control	6	CPu	100	123 ± 17.6	10.2 ± 1.14	6.42 ± 0.50	9.03 ± 0.84
vrDDfs	6	NAc	12.8	8.12 ± 2.03	1.40 ± 0.17	1.24 ± 0.24	n.d.
Control	6	NAc	100	63.6 ± 3.63	5.73 ± 0.29	6.03 ± 0.44	5.69 ± 0.66

DA, dopamine; HVA, homovanillic acid; DOPAC, 3.4-dihydroxyphenylacetic acid; 3-MT, 3-methoxytyramine. Data presented as means ± SEM (n.d. = none detected).

High-performance liquid chromatography (HPLC) coupled with electrochemical detection was used to measure monoamine content by the Neurochemistry Core Lab at Vanderbilt University's Center for Molecular Neuroscience Research (1). The brains of CO_2-asphyxiated mice were removed and placed on an ice-cold plate. Tissue cores (2.5-mm diameter) from the dorsal or ventral striata were taken from a 1-mm thick slice with the aid of a mouse brain matrix (Activational Systems, Warren, MI). The tissue was frozen in microcentrifuge tubes on dry ice and stored at -70°C.

1. Perez, F. A. & Palmiter, R. D. (2005) *Proc. Natl. Acad. Sci. USA* **102**, 2174-2179.

Table 2. Voltammetric quantification of evoked dopamine release

Group	*n*	Striatal subregion	Dorso-lateral	Dorso-medial	Ventro-lateral	Ventro-medial
DDfs	6	Dopamine concentration (μM)	n.d.	n.d.	n.d	n.d
	18	% sites w/ detectable release	0	0	0	0
vrDDfs	10	Dopamine concentration (μM)	0.43 ± 0.11	0.73 ± 0.25	0.41 ± 0.20	0.09 ± 0.04
	30	% sites w/ detectable release	83	90	53	53
Control	10	Dopamine concentration (μM)	1.76 ± 0.38	2.38 ± 0.37	2.53 ± 0.61	2.07 ± 0.57
	30	% sites w/ detectable release	100	100	93	93

For dopamine concentration and % sites w/ detectable release, *n* respectively indicates the number of unilateral slices (two per animal) and the number of release sites (three per region) examined.
Data are presented as means ± SEM (n.d. = no detectable dopamine current).

For voltammetric quantification of dopamine levels, mice were anesthetized with isoflurane and decapitated. The brain was removed and immersed in an ice-cold artificial cerebrospinal fluid (ACSF) containing (in mM): NaCl (119), KCl (2.5), MgSO4 (1.3), NaH2PO4 (1), NaHCO3 (26.2), CaCl2 (2.5), and D-glucose (11). Coronal slices 400-μm thick were cut with a vibrating microtome. A single slice from each animal was kept in ACSF (22°C); it was sectioned at the midline, and both halves were used. The ACSF was continuously bubbled with a gas mixture of 95% O_2 and 5% CO_2. Slices were left for 1 h before use. For recordings, the experimenter was blind to the genotype of the mouse from which slices were obtained. A slice was submerged in a small, illuminated chamber and perfused (2-3 mL/min) with ACSF warmed to 32° C. The tip of a carbon-fiber electrode (CFE; 7 μm in diameter, ≈50 μm in length) was gently lowered into the slice to a depth of 50-150 μm, and a bipolar, stainless steel stimulating electrode controlled by a stimulus isolation unit (Isoflex, AMPI, Jerusalem, Israel) was inserted about 100 μm from the CFE. Dopamine was detected at the CFE using fast-scan cyclic voltammetry (FSCV). The CFE was held at –0.4 V, and a triangular waveform (-0.4 to 1.3 V and back at 400 V/s, a total of 8.5 ms) was applied every 100 ms (10 Hz); signals were sampled at 117.65 kHz and low-pass filtered at 2 kHz. Stimulation consisted of 20 square pulses (0.1 ms, 1 mA, 50 Hz) delivered to each recording site twice, 120 s apart. Only the second event was analyzed. Background-subtracted cyclic voltammograms (current-voltage plots) were made by subtracting the average of the current recorded for 10 voltammetric scans (1 s) prior to stimulation from the current recorded for each voltammetric scan after stimulation. Changes in dopamine concentration were quantified by plotting the peak oxidation current (converted to dopamine concentration as described below) of the voltammograms corresponding to each 100-ms time point after stimulation. Recordings were made at three sites from in each of four striatal subregions in each slice. The four subregions were dorsolateral striatum, dorsomedial striatum, ventrolateral striatum and ventromedial striatum (the nucleus accumbens core ventral to the anterior commisure). The peak concentration of dopamine evoked at each recording site was averaged to give a single value for each subregion per slice. CFEs were calibrated at the end of a day of experiments to convert current to approximate dopamine concentration. The CFE tip was lowered into the end of the glass tube (1.1-mm inside diameter) from which ACSF perfused the slice. A 5-s “pulse” of 1 μM DA dissolved in oxygenated ACSF was allowed to pass through the perfusion tubing and over the CFE, and the current change was recorded with FSCV.